

Evolution of ferromagnetism in two-dimensional electron gas of $\text{LaTiO}_3/\text{SrTiO}_3$

Fangdi Wen,^{1,*} Yanwei Cao,^{1,2,†} Xiaoran Liu,¹ B. Pal,¹ S. Middey,³ M. Kareev,¹ and J. Chakhalian¹

¹*Department of Physics and Astronomy, Rutgers University, Piscataway, NJ 08854, USA*

²*Ningbo Institute of Materials Technology and Engineering,
Chinese Academy of Sciences, Ningbo, Zhejiang 315201, China*

³*Department of Physics, Indian Institute of Science, Bangalore 560012, India*

(Dated: February 28, 2018)

Understanding, creating, and manipulating spin polarization of two-dimensional electron gases at complex oxide interfaces presents an experimental challenge. For example, despite almost a decade long research effort, the microscopic origin of ferromagnetism in $\text{LaAlO}_3/\text{SrTiO}_3$ heterojunction is still an open question. Here, by using a prototypical two-dimensional electron gas (2DEG) which emerges at the interface between band insulator SrTiO_3 and antiferromagnetic Mott insulator LaTiO_3 , the experiment reveals the evidence for magnetic phase separation in hole-doped $\text{Ti } d^1 t_{2g}$ system resulting in spin-polarized 2DEG. The details of electronic and magnetic properties of the 2DEG were investigated by temperature-dependent d.c. transport, angle-dependent X-ray photoemission spectroscopy, and temperature-dependent magnetoresistance. The observation of clear hysteresis in magnetotransport at low magnetic fields implies spin-polarization from magnetic islands in the hole rich LaTiO_3 near the interface. These findings emphasize the role of magnetic instabilities in doped Mott insulators thus providing another path for designing all-oxide structures relevant to spintronics applications.

Utilizing the spin and charge degrees of freedom is a basic idea for spintronics applications, the study of which is fundamentally important for both basic science and device applications.¹⁻⁴ The past decade has witnessed a sharp rise of interest to complex oxide heterostructures and a great development of deposition techniques at the atomic scale,⁵⁻¹³ resulting in plethora of interesting phenomena emerging at complex oxide interfaces. In addition, those phenomena provide exciting opportunities for the design of all-oxide spintronics application and field-effect devices.¹⁴⁻¹⁹ Among these, understanding and control of two-dimensional electron gases (2DEGs) with spin-polarized carriers have attracted tremendous attention,¹⁸⁻³⁰ and yet remains a distinct challenge for the experimentalists.

In the past decade, the microscopic origin of ferromagnetism at $\text{LaAlO}_3/\text{SrTiO}_3$ has been actively investigated and yet not fully understood.³¹⁻³⁵ Specifically, since single crystal SrTiO_3 substrates with unavoidable defects and impurities can show some signature of ferromagnetism,³⁶ it is an open question whether the observation of ferromagnetism at the interfaces is an *intrinsic* property of 2DEG, or is more of a result of unavoidable defects/impurities from the sample preparation procedure.^{34,35} Alternatively, ferromagnetic layers have been used to induce the spin-polarization in 2DEGs. For example, ferromagnetic (FM) rare-earth titanate GdTiO_3 ($T_C \sim 32\text{K}$) was used as a charge/spin donor in $\text{GdTiO}_3/\text{SrTiO}_3$ heterojunctions^{25,26}, magnetic Co layer was shown to act as a spin injection source in multilayer heterostructure $\text{Co}/\text{LaAlO}_3/\text{SrTiO}_3$, and FM YTiO_3 layer was explicitly introduced in to 3-color $\text{YTiO}_3/\text{SrTiO}_3/\text{LaTiO}_3$ heterostructure.^{27,28} Following this route, one can naturally ask whether antiferromagnetic materials (e.g., Mott insulators LaTiO_3 , NdTiO_3 , and SmTiO_3) can induce spin-polarized 2DEGs in SrTiO_3 -based interfaces. However, recent works delivered a set of mixed answers, e.g. showing the absence of ferromagnetism in $\text{SmTiO}_3/\text{SrTiO}_3$ heterostructure,³⁷ and demonstrating the presence of ferromagnetism at the $\text{NdTiO}_3/\text{SrTiO}_3$ interface.³⁸ Moreover, no clear signature of ferromagnetism has been reported for the prototypical 2DEG of $\text{LaTiO}_3/\text{SrTiO}_3$.³⁹

To investigate this issue, we synthesized a series of high-quality $\text{SrTiO}_3/\text{LaTiO}_3$ (STO/LTO) heterostructures with variable thickness of the LaTiO_3 layer by pulsed laser deposition (PLD). The crystal structure was confirmed by X-ray diffraction (XRD) and the electronic and magnetic properties of 2DEG were investigated by temperature-dependent d.c. transport, Hall measurement, angle-dependent X-ray photoemission spectroscopy (XPS), and temperature-dependent magnetoresistance (MR). The combination of probes revealed clear hysteretic behavior of MR is only observed at the interfaces of STO/LTO with thicker LTO layer (20 u.c.) and absent for the thinner LaTiO_3 layer (3 u.c.). Based on the observation we conjecture how the FM behavior of 2DEG can be resulted from the spin-flip scattering between conduction electrons and magnetic islands with localized electrons, with an additional contribution to canted ferromagnetism from the inner antiferromagnetic atomic planes of LTO layer. Our results show alternative way to control the magnetism of 2DEGs in titanate-based interfaces and should be important for designing all-oxide-based spintronics.

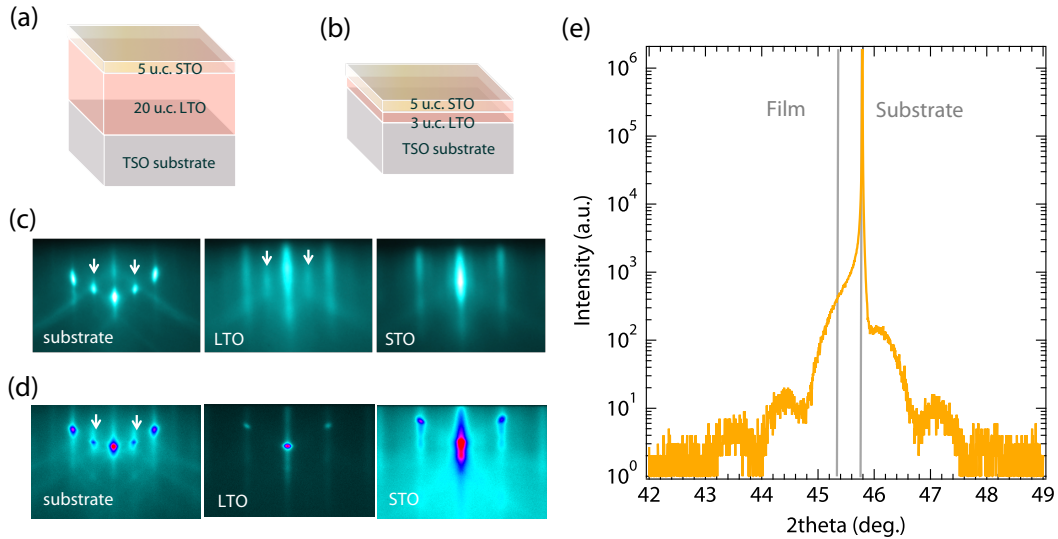


FIG. 1. (a) and (b) Sketch of $5\text{u.c. SrTiO}_3/n\text{u.c. LaTiO}_3$ ($n = 20$ and 3 , u.c. = unit cells) heterostructures on TbScO_3 substrates. (c) RHEED patterns of $5\text{STO}/20\text{LTO}$ during growth for TbScO_3 substrate, LaTiO_3 , and SrTiO_3 , respectively. Yellow arrows indicate the half-order-peaks. (d) RHEED patterns of $5\text{STO}/3\text{LTO}$ during growth. (e) XRD of $5\text{STO}/20\text{LTO}$ sample. The intensity is plotted on a log scale, and the film peak is to the left of substrate peak.

As shown in inset of Fig. 1. (a) and (b), in all the designed samples, STO is a top layer and grown on the thicker LTO layer resulting in the 2DEG formed at the STO/LTO interface. Specifically, high-quality $5\text{u.c. SrTiO}_3/n\text{u.c. LaTiO}_3$ ($n = 3, 20, 5\text{STO}/n\text{LTO}$ after, and u.c. = unit cells) heterostructures on TbScO_3 (110)-oriented (orthorhombic notation) single crystal substrates ($5 \times 5 \times 0.5\text{ mm}^3$) were epitaxially synthesized by PLD using a KrF excimer laser operating at $\lambda = 248\text{ nm}$ and 2 Hz pulse rate. These stated growth condition can be found in our previous reports.^{23,24} Figures 1 (c)-(d) exhibit typical *in-*

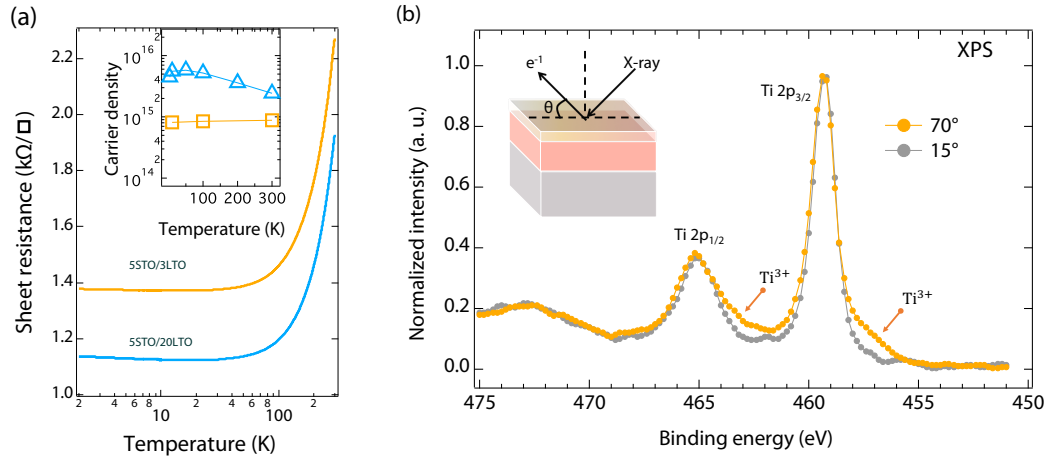


FIG. 2. (a) Temperature-dependent sheet resistances of 5STO/20LTO and 5STO/3LTO. (b) Angle-dependent Ti $2p$ core level XPS on 5STO/20LTO at room temperature. θ is the angle between sample surface and the axis of acceptance angle of electron energy analyzer.

situ RHEED patterns with distinct specular and off-specular reflections distributed on the Laue rings which attest for the high crystallinity and flatness of the heterostructures. Notice, the growth sequence of 5STO/ n LTO samples is quite different from the previously reported results in which LTO is always the top layer grown on STO substrates.^{40–42} The main reason for the inverted layer sequence (i.e. STO/LTO vs. LTO/STO) is two-fold. First, the surface of antiferromagnetic LTO can be easily oxidized and becomes paramagnetic $\text{LaTiO}_{3+\delta}$.⁴³ In addition, as previously reported the STO substrate itself can host metallicity and magnetism.^{36,44} To avoid this, STO is replaced by inert TbScO_3 in our samples. Structural properties of the film were further investigated by high-resolution X-ray diffraction (XRD) in the vicinity of TSO (002) reflection. As shown in Fig. 1(e), left to the sharp peak of the substrate, the broad (002) reflection of the film is clearly observed with well-defined Kiessig fringes. From the angular interval of the fringes, the total thickness of the film is determined ~ 9.31 nm. This result agrees well with the estimated value according to the numbers of intensity oscillations of RHEED during the deposition, corroborating the high quality of the film.

With the availability of high quality samples, we have investigated in detail the properties of 2DEG in 5STO/ n LTO ($n = 3$ and 20). First, to confirm the formation of a 2DEG, temperature-dependent resistance measurements were carried out. As shown in Fig. 2 (a), the sheet resistance of the 5STO/20LTO sample decreases from ~ 1.9 kΩ/□ at 300 K to ~ 1.1 kΩ/□ at 2 K, indicating a typically metallic behavior. Similarly, as expected, the temperature dependent resistivity of 5STO/3LTO also shows metallic behavior in the same T -range. The existence of 2DEG was proved by measuring Hall effect on both 5STO/20LTO and 5STO/3LTO sample in different temperature. By plotting the temperature dependence of carrier density, we got a carrier density close to $4 \times 10^{15} \text{ cm}^{-2}$ for 5STO/20LTO and $8 \times 10^{14} \text{ cm}^{-2}$ for 5STO/3LTO stable under changing temperature. This data is close to the estimated carrier density $3 \times 10^{14} \text{ cm}^{-2}$ for half electron doping. This number does not change a lot when the temperature changes, which is also a typical property of 2DEG, as shown in the inset of Fig. 2. (a). To further investigate the electronic structure near the interface of 5STO/20LTO, we performed angle-dependent XPS measurements. Fig. 2. (b) shows typical Ti $2p$ core level spectra acquired at two acceptance angles of the analyzer. Due to the small value of the inelastic mean free path (~ 1.5 nm for 1 keV),⁴⁵ the probing depth is extremely close to the surface for small angle ($\theta = 15^\circ$), while for the larger angle ($\theta = 75^\circ$), it is more sensitive to deeper parts of the structure. As seen in Fig. 2. (b), the main two features near 459.3 eV and 465.2 eV can be assigned to Ti^{4+} $2p_{3/2}$ and $2p_{1/2}$ peaks, respectively.²⁵ Most importantly, in contrast to the small-angle spectra ($\theta = 15^\circ$, surface sensitive), the spectra acquired at $\theta = 70^\circ$ exhibit two pronounced shoulders near 457 eV and 463 eV (marked by arrows in Fig. 2.(b)). Those energy positions corresponds to the contribution of Ti^{3+} $2p_{3/2}$ and $2p_{1/2}$ peaks.²⁵ The relative intensity of Ti^{3+} increases as we go from lower to higher angle. It suggests that the surface is more Ti^{4+} rich and the relative concentration of Ti^{3+} increases as with go deep inside the film. These results are consistent with our sample design as 5 u.c. of SrTiO_3 is deposited on top of 20 u.c. LaTiO_3 in this bi-layer system.

Next, we explore the magnetic properties of 5STO/ n LTO. Figure 3 shows the magnetoresistance (MR) data for 5STO/20LTO taken from 2K to 5 K with an applied external magnetic field along in-plane and out-of-plane directions, respectively. As seen in Fig. 3(a), in sharp contrast to the conventional positive magneto-resistance in 5STO/3LTO, a clear hysteresis was found in 5STO/20LTO with out-of-plane magnetic field at 2 K. This emergent feature is surprising considering that the thickness is the only changed factor. In order to gain further insight into this phenomenon, we measured temperature-dependent magneto-resistance on 5STO/20LTO with both out-of-plane (Fig. 3(b)) and in-plane (Fig. 3(c)) magnetic fields. As shown in Fig. 3(c), besides the usual positive magneto-resistance above 1.5 T, the dominant feature here is the presence of hysteresis under the moderate magnetic fields, implying the formation of ferromagnetism in 2DEG.^{31,32,38} Interestingly, unlike a simple line shape

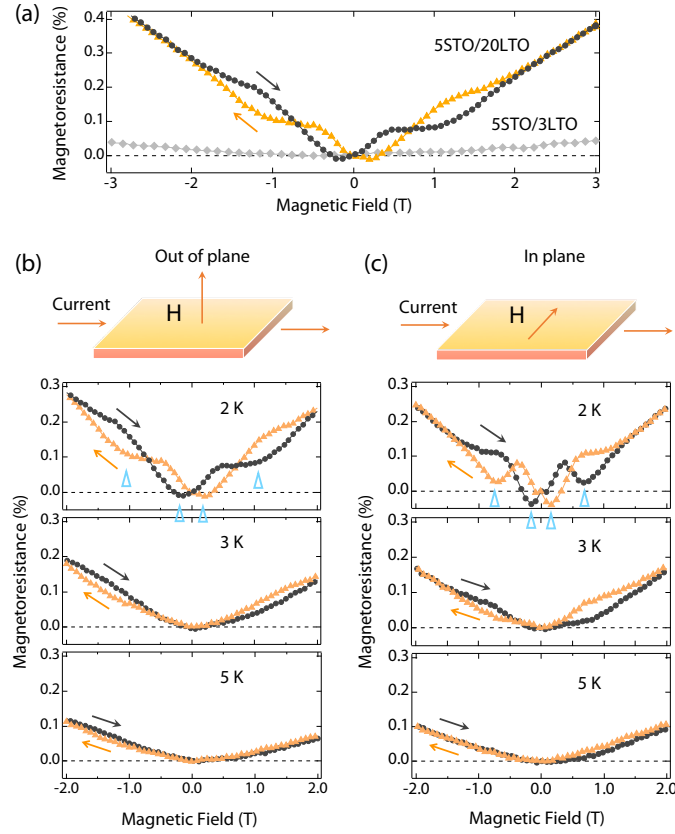


FIG. 3. (a) Comparison of magnetoresistance between 5STO/20LTO and 5STO/3LTO heterostructures at temperature 2 K with out-of-plane magnetic field. (b) and (c) Temperature-dependent magnetoresistance of 5STO/20LTO with out-of-plane and in-plane magnetic fields, respectively. Black and orange arrows indicate the sweep directions of the external magnetic field, whereas blue triangles mark the critical magnetic field of magnetoresistance. Here, the magnitude of magnetoresistance (MR) is defined as $MR = [R(H) - R(0)] / R(0) \times 100 \%$, where $R(H)$ represents the sheet resistance under external field H .

of hysteresis reported for $\text{SrTiO}_3/\text{NdTiO}_3$,³⁸ our heterostructure shows a more complex line shape with two critical magnetic fields of $\sim \pm 0.2$ and ± 0.7 T (marked by blue triangles in Fig. 3(c) at 2 K). Upon increasing the temperature from 2 to 3 K, the hysteresis becomes strongly suppressed but the second critical field of $\sim \pm 0.7$ T still survives. This feature disappears completely once the temperature exceeds 5 K. The observed MR behavior under out-of-plane magnetic field [Fig. 3(b)] is analogous to that of in-plane magnetic field [Fig. 3(c)].

In general, MR can be attributed to various sources including the Lorentz force, spin scattering, anisotropy, weak localization, and so on.⁴⁶ As well known, with the application of an external magnetic field, the Lorentz force can reduce the mobility of conduction carriers and increase the amplitude of sheet resistance, resulting in a classical positive and non-saturating magnetoresistance; In this mechanism, $MR \sim H^2$.⁴⁷ As clearly seen in Fig. 3, the effect of Lorentz force is distinct for the field larger than 2 T, giving rise to the parabolic MR contribution. On the other hand, under low magnetic field the contribution of spin scattering becomes significant leading to the hysteretic behavior of MR.³¹ From the similarity between the line shape of MR under in- and out-of-plane magnetic field [Fig. 3(b) and 3(c)] we can rule out the leading effect of anisotropy for observed hysteresis.

Other than general factors, we discussed a possible microscopic origin of spin polarization (or ferromagnetism) in the 2DEG in 5STO/20LTO. The observed hysteric MR may arise from two contributions: (1) the spin-flip scattering between 2DEG and magnetic islands formed near the interface and (2) the magnetic interaction of 2DEG with canted ferromagnetism from LTO layers. Theoretically, it has been predicted that in a hole doped $3d^1 t_{2g}$ Mott insulator (e.g. LaTiO_3 or YTiO_3) away from half-filling, the system becomes thermodynamically unstable which results in a phase separation into antiferromagnetic, ferromagnetic or paramagnetic Fermi liquid regions depending on the doping level.^{48,49} Furthermore, it has been proposed that in the case of $\text{SrTiO}_3/\text{NdTiO}_3$ the phase-separation mechanism may transfer such spin-polarization into 2DEG.³⁸ Similar to the conclusion people got in the $\text{SrTiO}_3/\text{NdTiO}_3$ system, as schematically shown in Fig. 4, due to interfacial charge transfer from LTO into STO layers, the Ti $3d$ band is less than half filled in $\text{LaTi}^{(3+/4+)}\text{O}_3$. This less than half filled band structure in turn leads to the phase separation in hole-doped Mott insulator $\text{LaTi}^{(3+/4+)}\text{O}_3$ with ferro- or ferrimagnetic islands formed near the STO/LTO interface.⁴⁹ However, when the thickness of the LTO layer approaches its ultra thin limit, the doping level was ef-

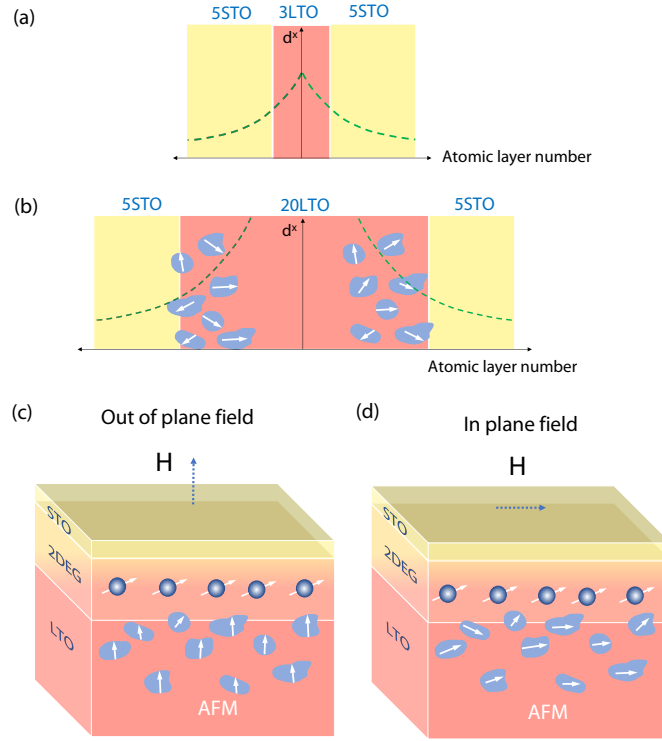


FIG. 4. (a) Schematic of charge decay of 5STO/3LTO. (b) Schematic of charge decay of 5STO/20LTO with the formation of magnetic islands in LaTiO_3 layers. (c) and (d) Schematic of origin of spin-polarized 2DEG (blue balls) in 5STO/20LTO interface with out-of-plane and in-plane magnetic fields, respectively. Blue domains show magnetic islands with random moment near the interface, whereas the white arrows mark the directions of magnetic moments.

fectively increased, and the hole-doped LTO will favor paramagnetic Fermi liquid. This explains the absence of hysteresis in 5STO/3LTO (see Fig. 4 (a)). On the other hand, for 5STO/20LTO whose LTO layer is significantly thicker (20 u. c. vs. 3 u. c.), the spin-flip scattering between conduction electrons and magnetic islands can mediate the spin-polarization in 2DEG, (see Fig.s 4(b)-(d)).^{38,51,52} As shown in Fig. 4. (c), after application of the external magnetic field, the orientation of magnetic moments in the magnetic islands is expected to follow the direction of the magnetic field in both in-plane and out-of-plane case, which is consistent with the observation of isotropic critical field of $\sim \pm 0.2$ T for both in- and out-of-plane magnetic fields. In addition to the unconventional MR , the other interesting feature is the prepresence of extra minima. The canting of the AFM ordering affect the distribution and orientation of the magnetic islands that interact with the mobile electrons at the interface, and leads to a peak shift of the additional dip. Specifically, when we applied out-of-plane field, the different dip location (~ 1 T for out of plane whereas ~ 0.7 T for in-plane) indicates the anisotropic axis of the spins in LTO tends to align more along the out-of-plane direction.⁵²

In summary, we report on the evolution of ferromagnetism in the 2DEG formed at the interface of 5STO/ n LTO ($n=20$ and 3) heterostructures. The RHEED and XRD were present to confirm our crystal structure, and temperature-dependent electrical transport, Hall effect and angle-dependent XPS were performed to characterize the mixed valency of $\text{Ti}^{3+/4+}$ near the interface of STO/LTO. By measuring temperature-dependent magnetoresistance, we revealed the presence of clear hysteresis of magnetoresistance, implying the spin polarization of 2DEG in 5STO/20LTO. This ferromagnetic behavior of the 2DEG can be attributed primarily to the spin-flip scattering between conduction carriers, ferro- or ferri- magnetic islands and canted antiferromagnetism near the interface. Our results emphasize the importance and phase instability for the correlated oxide interfaces which is directly relevant for designing all-oxide spintronics applications based on doped Mott materials.

Acknowledgements

F. W. was supported by the Claud Lovelace Graduate Fellowship. Y. C. acknowledged the Gordon and Betty Moore Foundations' EPIQS Initiative through ICAM-I2CAM, Grant GBMF5305. X. L. was supported by the Department of Energy Grant No. DE-SC0012375. J. C. acknowledged the support by the Gordon and Betty Moore Foundation EPIQS Initiative through Grant

-
- * fw113@physics.rutgers.edu
† ywcao@nimte.ac.cn
- ¹ I. Žutić, J. Fabian, and S. Das Sarma, *Rev. Mod. Phys.* **76**, 323 (2004).
 - ² S. D. Bader and S. S. P. Parkin, *Annu. Rev. Condens. Matter Phys.* **1**, 71 (2010).
 - ³ F. Pulizzi, *Nat. Mater.* **11**, 367 (2012).
 - ⁴ M. Eschrig, *Rep. Prog. Phys.* **78**, 104501 (2015).
 - ⁵ H. Y. Hwang, Y. Iwasa, M. Kawasaki, B. Keimer, N. Nagaosa, and Y. Tokura, *Nat. Mater.* **11**, 103 (2012).
 - ⁶ J. Chakhalian, A. J. Millis, and J. Rondinelli, *Nat. Mater.* **11**, 92 (2012).
 - ⁷ J. Chakhalian, J. W. Freeland, A. J. Millis, C. Panagopoulos, and J. M. Rondinelli, *Rev. Mod. Phys.* **86**, 1189 (2014).
 - ⁸ M. Lorenz, M. S. Ramachandra Rao, T. Venkatesan, E. Fortunato, P. Barquinha, R. Branquinho, D. Salgueiro, R. Martins, E. Carlos, A. Liu, F. K. Shan, M. Grundmann, H. Boschker, J. Mukherjee, M. Priyadarshini, N. DasGupta, D. J. Rogers, F. H. Teherani, E. V. Sandana, P. Bove, K. Rietwyk, A. Zaban, A. Veziridis, A. Weidenkaff, M. Muralidhar, M. Murakami, S. Abel, J. Fompeyrine, J. Zuniga-Perez, R. Ramesh, N. A. Spaldin, S. Ostanin, V. Borisov, I. Mertig, V. Lazenka, G. Srinivasan, W. Prellier, M. Uchida, M. Kawasaki, R. Pentcheva, P. Gegenwart, F. Miletto Granozio, J. Fontcuberta, and N. Pryds, *J. Phys. D: Appl. Phys.* **49**, 433001 (2016).
 - ⁹ F. M. Granozio, G. Koster, and G. Rijnders, *MRS Bull.* **38**, 1017 (2013).
 - ¹⁰ S. Stemmer and S. J. Allen, *Annu. Rev. Mater. Res.* **44**, 151 (2014).
 - ¹¹ J. Mannhart, D. H. A. Blank, H. Y. Hwang, A. J. Millis, and J.-M. Triscone, *MRS Bull.* **33**, 1027 (2008).
 - ¹² L. Bjaalie, B. Himmetoglu, L. Weston, A. Janotti, and C. G. Van de Walle, *New J. Phys.* **16**, 025005 (2014).
 - ¹³ D. G. Schlom, L.-Q. Chen, C.-B. Eom, K. M. Rabe, S. K. Streiffer, and J.-M. Triscone, *Annu. Rev. Mater. Res.* **37**, 589 (2007).
 - ¹⁴ J. Mannhart and D. G. Schlom, *Science* **327**, 1607 (2010).
 - ¹⁵ M. Bibes and A. Barthélémy, *IEEE Trans. Electron Devices* **54**, 1003 (2007).
 - ¹⁶ M. C. Prestgard, G. P. Siegel, and A. Tiwari, *Adv. Mat. Lett.* **5**, 242 (2014).
 - ¹⁷ C. Woltmann, T. Harada, H. Boschker, V. Srot, P. A. van Aken, H. Klauk, and J. Mannhart, *Phys. Rev. Applied* **4**, 064003 (2015).
 - ¹⁸ F. Hellman, A. Hoffmann, Y. Tserkovnyak, G. S. D. Beach, E. E. Fullerton, C. Leighton, A. H. MacDonald, D. C. Ralph, D. A. Arena, H. A. Dürr, P. Fischer, J. Grollier, J. P. Heremans, T. Jungwirth, A. V. Kimel, B. Koopmans, I. N. Krivorotov, S. J. May, A. K. Petford-Long, J. M. Rondinelli, N. Samarth, I. K. Schuller, A. N. Slavin, M. D. Stiles, O. Tchernyshyov, A. Thiaville, and B. L. Zink, *Rev. Mod. Phys.* **89**, 025006 (2017).
 - ¹⁹ N. Reyren, M. Bibes, E. Lesne, J.-M. George, C. Deranlot, S. Collin, A. Barthélémy, and H. Jaffrès, *Phys. Rev. Lett.* **108**, 186802 (2012).
 - ²⁰ J. Betancourt, T. R. Paudel, E. Y. Tsymlal, and J. P. Velev, *Phys. Rev. B* **96**, 045113 (2013).
 - ²¹ R. Ohshima, Y. Ando, K. Matsuzaki, T. Susaki, M. Weiler, S. Klingler, H. Huebl, E. Shikoh, T. Shinjo, S. T. B. Goennenwein, and M. Shiraishi, *Nat. Mater.* **16**, 609 (2017).
 - ²² W. M. Lü, S. Saha, X. R. Wang, Z. Q. Liu, K. Gopinadhan, A. Annadi, S. W. Zeng, Z. Huang, B. C. Bao, C. X. Cong, M. Venkatesan, T. Yu, J. M. D. Coey, Ariando, and T. Venkatesan, *Nat. Commun.* **7**, 11015 (2016).
 - ²³ M. Kareev, Y. Cao, X. Liu, S. Middey, D. Meyers, and J. Chakhalian, *Appl. Phys. Lett.* **103**, 231605 (2013).
 - ²⁴ Y. Cao, Z. Yang, M. Kareev, X. Liu, D. Meyers, S. Middey, D. Choudhury, P. Shafer, J. Guo, J. W. Freeland, E. Arenholz, L. Gu, and J. Chakhalian, *Phys. Rev. Lett.* **116**, 076802 (2016).
 - ²⁵ P. Moetakef, J. Y. Zhang, A. Kozhanov, B. Jalan, R. Seshadri, S. J. Allen, and S. Stemmer, *Appl. Phys. Lett.* **98**, 112110 (2011).
 - ²⁶ C. A. Jackson and S. Stemmer, *Phys. Rev. B* **88**, 180403(R) (2013).
 - ²⁷ A. G. Swartz, S. Harashima, Y. Xie, D. Lu, B. Kim, C. Bell, Y. Hikita, and H. Y. Hwang, *Appl. Phys. Lett.* **105**, 032406 (2014).
 - ²⁸ H. Inoue, A. G. Swartz, N. J. Harmon, T. Tachikawa, Y. Hikita, M. E. Flatté, and H. Y. Hwang, *Phys. Rev. X* **5**, 041023 (2015).
 - ²⁹ J. X. Duan, N. Tang, J. D. Ye, F. H. Mei, K. L. Teo, Y. H. Chen, W. K. Ge, and B. Shen, *Appl. Phys. Lett.* **102**, 192405 (2013).
 - ³⁰ A. Narjis, A. El kaaouachi, C.-T. Liang, L. Limouny, S. Dlimi, A. Sybous, M. Errai, and E. Daoudi, *Phys. Scr.* **87**, 045703 (2013).
 - ³¹ A. Brinkman, M. Huijben, M. V. Zalk, J. Huijben, U. Zeitler, J. C. Maan, W. G. van der Wiel, G. Rijnders, D. H. A. Blank, and H. Hilgenkamp, *Nat. Mater.* **6**, 493 (2007).
 - ³² D. A. Dikin, M. Mehta, C. W. Bark, C. M. Folkman, C. B. Eom, and V. Chandrasekhar, *Phys. Rev. Lett.* **107**, 056802 (2011).
 - ³³ Ariando, X. Wang, G. Baskaran, Z. Q. Liu, J. Huijben, J. B. Yi, A. Annadi, A. Roy Barman, A. Rusydi, S. Dhar, Y. P. Feng, J. Ding, H. Hilgenkamp, and T. Venkatesan, *Nat. Commun.* **2**, 188 (2011).
 - ³⁴ B. Kalisky, J. A. Bert, B. B. Klopfer, C. Bell, H. K. Sato, M. Hosoda, Y. Hikita, H. Y. Hwang, and K. A. Moler, *Nat. Commun.* **3**, 922 (2012).
 - ³⁵ M. R. Fitzsimmons, N. W. Hengartner, S. Singh, M. Zhernenkov, F. Y. Bruno, J. Santamaria, A. Brinkman, M. Huijben, H. J. A. Molegraaf, J. de la Venta, and Ivan K. Schuller, *Phys. Rev. Lett.* **107**, 217202 (2011).
 - ³⁶ J. M. D. Coey, M. Venkatesan, and P. Stamenov, *J. Phys.: Condens. Matter* **28**, 485001 (2016).
 - ³⁷ C. A. Jackson, J. Y. Zhang, C. R. Freeze, and S. Stemmer, *Nat. Commun.* **5**, 4258 (2014).
 - ³⁸ Y. Ayino, P. Xu, J. Tigre-Lazo, J. Yue, B. Jalan, and V. S. Pribiag, *arXiv: 1704.08828* (2017).
 - ³⁹ A. Ohtomo, D. A. Muller, J. L. Grazul, H. Y. Hwang, *Nature* **419**, 378 (2002).
 - ⁴⁰ A. Rastogi, J. J. Pulikkotil, S. Auluck, Z. Hossain, and R. C. Budhani, *Phys. Rev. B* **86**, 075127 (2012).
 - ⁴¹ J. Biscaras, N. Bergeal, A. Kushwaha, T. Wolf, A. Rastogi, R. C. Budhani, and J. Lesueur, *Nat. Commun.* **1**, 89 (2010).
 - ⁴² F. J. Wong, S.-H. Baek, R. V. Chopdekar, V. V. Mehta, H.-W. Jang, C.-B. Eom, and Y. Suzuki, *Phys. Rev. B* **81**, 161101(R) (2010).

- ⁴³ Y. Taguchi, T. Okuda, M. Ohashi, C. Murayama, N. Môri, Y. Iye, and Y. Tokura, Phys. Rev. B **59**, 7917 (1999).
- ⁴⁴ X. Lin, G. Bridoux, A. Gourgout, G. Seyfarth, S. Krämer, M. Nardone, B. Fauqué, and K. Behnia, Phys. Rev. Lett. **112**, 207002 (2014).
- ⁴⁵ B. Da, H. Shinotsuka, H. Yoshikawa, Z. J. Ding, and S. Tanuma, Phys. Rev. Lett. **113**, 063201 (2014).
- ⁴⁶ P. Stamenov, M. Venkatesan, L. S. Dorneles, D. Maude, and J. M. D. Coey, J. Appl. Phys. **99**, 08M124 (2006).
- ⁴⁷ G. Giuliani, EPL **81**, 60002 (2008).
- ⁴⁸ C.-H. Yee and L. Balents, Phys. Rev. X **5**, 021007 (2015).
- ⁴⁹ D. Khomskii, *Basic Aspects of the Quantum Theory of Solids: Order and Elementary Excitations*. (Cambridge University Press), pp. 247-251.
- ⁵⁰ G. Allodi, R. De Renzi, G. Guidi, F. Licci, and M. W. Pieper, Phys. Rev. B **56**, 6036 (1997).
- ⁵¹ M. R. Boon, Phys. Rev. B **7**, 761 (1973).
- ⁵² M. Mehta, D. A. Dikin, C. W. Bark, S. Ryu, C. M. Folkman, C. B. Eom, and V. Chandrasekhar, Nat. Commun. **3**, 955 (2012).